Global optimal attitude estimation using uncertainty ellipsoids

Amit K. Sanyal[a,*], Taeyoung Lee[b], Melvin Leok[c], N. Harris McClamroch[c]

[a]*Department of Mechanical Engineering, University of Hawaii, Honolulu, HI 96822, USA*
[b]*Department of Aerospace Engineering, University of Michigan, Ann Arbor, MI 48109-2140, USA*
[c]*Department of Mathematics, Purdue University, West Lafayette, IN 47907-2067, USA*

Abstract

A deterministic attitude estimation problem for a rigid body in a potential field, with bounded attitude and angular velocity measurement errors is considered. An attitude estimation algorithm that globally minimizes the attitude estimation error is obtained. Assuming that the initial attitude, the initial angular velocity and measurement noise lie within given ellipsoidal bounds, an uncertainty ellipsoid that bounds the attitude and the angular velocity of the rigid body is obtained. The center of the uncertainty ellipsoid provides point estimates, and the size of the uncertainty ellipsoid measures the accuracy of the estimates. The point estimates and the uncertainty ellipsoids are propagated using a Lie group variational integrator and its linearization, respectively. The attitude and angular velocity estimates are optimal in the sense that the sizes of the uncertainty ellipsoids are minimized.
Published by Elsevier B.V.

Keywords: Global attitude representation; Deterministic estimation; Uncertainty ellipsoids

1. Introduction

Attitude estimation is often a prerequisite for controlling aerospace and underwater vehicles, mobile robots, and other mechanical systems moving in space. In this paper, we study the attitude estimation problem for the uncontrolled dynamics of a rigid body in an attitude-dependent force potential (like uniform gravity). The estimation scheme we present has the following important features: (1) the attitude is globally represented without using any coordinate system, (2) the filter obtained is not a Kalman or extended Kalman filter and (3) the attitude and angular velocity measurement errors are assumed to be bounded, with known ellipsoidal uncertainty bounds. The static attitude estimation scheme presented here is based on [22]. The attitude is represented globally using proper orthogonal matrices and the exponential map on the set of 3×3 skew-symmetric matrices. Such a global representation has been recently used for partial attitude estimation with a linear dynamics model

in [20]. The uncertainty ellipsoids are represented in terms of local charts that are based at the current estimated attitude, and as such do not suffer from the coordinate singularities that arise when attempting to represent uncertainties using only a single chart based at the initial attitude, as is typical for competing approaches. The estimation scheme presented here is deterministic, based on known measurement uncertainty bounds propagated by the dynamic flow.

The attitude determination problem for a rigid body from vector measurements was first posed in [28]. A sample of the literature in spacecraft attitude estimation can be found in [7,2,17,24,25]. Applications of attitude estimation to unmanned vehicles and robots can be found in [20,3,21,27]. Most existing attitude estimation schemes use generalized coordinate representations of the attitude. As is well known, minimal coordinate representations of the rotation group, like Euler angles, Rodrigues parameters, and modified Rodrigues parameters (see [8]), usually lead to geometric or kinematic singularities. Non-minimal coordinate representations, like the unit quaternions used in the quaternion estimation (QUEST) algorithm [24] and its several variants [2,19,25], have their own associated problems. Besides the extra constraint of unit norm that one needs to impose, the quaternion vector itself can be defined in one

* Corresponding author. Tel.: +1 808 956 2142.
E-mail addresses: aksanyal@hawaii.edu (A.K. Sanyal), tylee@umich.edu (T. Lee), mleok@math.purdue.edu (M. Leok), nhm@umich.edu (N.H. McClamroch).

of two ways, depending on the sense of rotation used to define the principal angle.

A brief outline of this paper is given here. In Section 2, the attitude determination problem for vector measurements with measurement noise is introduced, and a global attitude determination algorithm which minimizes the attitude estimation error is presented. The attitude dynamics and dynamic estimation problem is formulated for a rigid body in an attitude-dependent potential. Section 3 presents the attitude estimation scheme assuming that both attitude and angular velocity measurements are available simultaneously. Sufficient conditions for convergence of the estimates are given. This attitude estimation scheme has also been extended and applied to the case where only attitude but no angular velocity measurements are available, and recently reported in [14]. Section 4 presents concluding remarks and observations.

2. Attitude estimation from vector observations

Attitude of a rigid body is defined as the orientation of a body fixed frame with respect to an inertial reference frame; it is represented by a rotation matrix that is a 3×3 orthogonal matrix with determinant $+1$. Rotation matrices have a group structure denoted by SO(3), and its action on $\mathbb{R}^3$ takes a vector represented in body fixed frame into its representation in the reference frame by matrix multiplication.

2.1. Attitude determination procedure

We assume that there are m fixed points in the spatial reference frame, no two of which are co-linear, that are measured in the body frame. We denote the known direction of the ith point in the spatial reference frame as $e^i \in \mathbb{S}^2$ where $\mathbb{S}^2$ denotes the two sphere (embedded in $\mathbb{R}^3$). The corresponding vector is represented in the body fixed frame as $b^i \in \mathbb{S}^2$. Since we only measure directions, we normalize e^i and b^i so that they have unit lengths. The e^i and b^i are related by a rotation matrix $C \in$ SO(3) that defines the attitude of the rigid body;

$$e^i = Cb^i$$

for all $i \in \{1, 2, \ldots, m\}$. We assume that e^i is known accurately and we assume that b^i is measured in the body fixed frame. Let the measured direction vector be $\tilde{b}^i \in \mathbb{S}^2$, which contains measurement errors, and let an estimate of the rotation matrix be $\widehat{C} \in$ SO(3). The vector estimation errors are given by

$$e^i - \widehat{C}\tilde{b}^i, \quad i = 1, \ldots, m.$$

The weighted 2 norm of these errors is given by the error functional,

$$\mathcal{J}(\widehat{C}) = \frac{1}{2} \sum_{i=1}^{m} w_i (e^i - \widehat{C}\tilde{b}^i)^{\mathrm{T}} (e^i - \widehat{C}\tilde{b}^i),$$

$$= \frac{1}{2} \mathrm{tr}[(E - \widehat{C}\tilde{B})^{\mathrm{T}} W (E - \widehat{C}\tilde{B})],$$

where $E = [e^1, e^2, \ldots, e^m] \in \mathbb{R}^{3 \times m}$, $\tilde{B} = [\tilde{b}^1, \tilde{b}^2, \ldots, \tilde{b}^m] \in \mathbb{R}^{3 \times m}$, and $W = \mathrm{diag}[w^1, w^2, \ldots, w^m] \in \mathbb{R}^{m \times m}$ has a

weighting factor for each measurement. We assume that $m \geqslant 3$ in this paper. If $m = 2$, we can take the cross-product of the two measured unit vectors $\tilde{b}^1 \times \tilde{b}^2 = \tilde{b}^3$ and treat that as a third measured direction, with the corresponding unit vector in the inertial frame taken to be $e^3 = e^1 \times e^2$. The attitude determination problem then consists of finding $\widehat{C} \in$ SO(3) such that the error functional $\mathcal{J}$ is minimized:

$$\widehat{C} = \arg \min_{\tilde{C} \in \mathrm{SO}(3)} \mathcal{J}(\tilde{C}). \tag{1}$$

The problem (1) is known as Wahba's problem [28]. The original solution of Wahba's problem is given in [11], and a solution expressed in terms of quaternions, known as the QUEST algorithm, is presented in [24]. A solution without using generalized attitude coordinates is given in [24]. A necessary condition for optimality of (1) is given in [22] as

$$L^{\mathrm{T}}\widehat{C} = \widehat{C}^{\mathrm{T}}L, \tag{2}$$

where $L = EW\widetilde{B}^{\mathrm{T}} \in \mathbb{R}^{3 \times 3}$.

The following result, proved in [22], gives an unique estimate $\widehat{C} \in$ SO(3) of the attitude matrix that satisfies (2) and solves the attitude determination problem (1).

Theorem 2.1. *The unique minimizing solution to the attitude determination problem* (1) *is given by*

$$\widehat{C} = SL, \quad S = Q\sqrt{(RR^{\mathrm{T}})^{-1}}Q^{\mathrm{T}}, \tag{3}$$

where

$$L = QR, \quad Q \in \mathrm{SO}(3) \tag{4}$$

and R is upper triangular and invertible; this is the QR decomposition of L. The symmetric positive definite (principal) square root is used in (3).

Proof. Using the QR decomposition of L given by (4), we can express the orthogonality condition of $\widehat{C}$ as follows:

$$\widehat{C}\widehat{C}^{\mathrm{T}} = SQRR^{\mathrm{T}}Q^{\mathrm{T}}S = I_3.$$

Due to the necessary condition (2), S is symmetric since $L^{\mathrm{T}}\widehat{C} = L^{\mathrm{T}}SL$ is symmetric. The sufficient condition for $\widehat{C}$ to minimize cost function $\mathcal{J}$, is obtained by taking its second variation with respect to $\widehat{C}$. The following sufficient condition is obtained in [22]:

$$\delta^2_{\widehat{C}} \mathcal{J} = -\mathrm{tr}[(L^{\mathrm{T}}\widehat{C}U^2)] > 0. \tag{5}$$

It is shown in [22] that the sufficient condition (5) is equivalent to $D = L^{\mathrm{T}}\widehat{C}$ being positive definite, i.e., $v^{\mathrm{T}}Dv > 0$ for any $v \in \mathbb{R}^3$. This in turn is equivalent to $S = (L^{\mathrm{T}})^{-1}DL^{-1}$ being positive definite.

Therefore, S is given by

$$S = \sqrt{Q(RR^{\mathrm{T}})^{-1}Q^{\mathrm{T}}} = Q\sqrt{(RR^{\mathrm{T}})^{-1}}Q^{\mathrm{T}},$$

where the principal (positive definite) square root is taken, as given by Eq. (3). This makes S positive definite, as required by
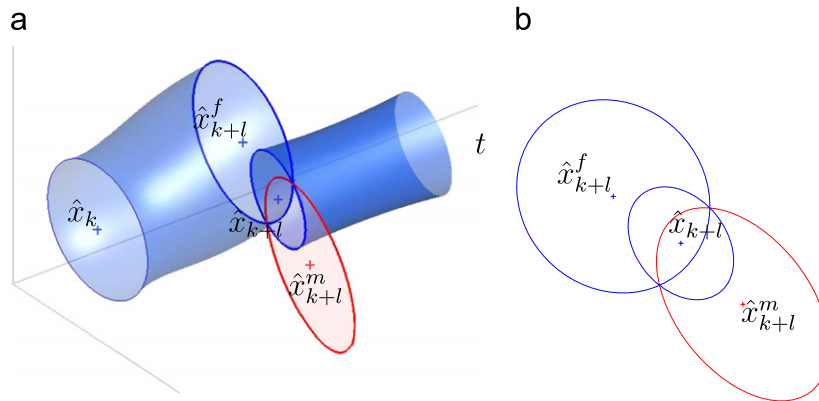
Fig. 1. Uncertainty ellipsoids. (a) Propagation of uncertainty ellipsoid. (b) Filtering procedure.

Eq. (5). By construction, $\widehat{C} = SL$ satisfies $\widehat{C}\widehat{C}^T = I_3$. Now we check the determinant of $\widehat{C} = SL$:

$$\det \widehat{C} = \det S \det L$$

$$= \left(\det Q^T \det \sqrt{(RR^T)^{-1}} \det Q \right) (\det Q \det R)$$

$$= \frac{(\det Q)^2}{\sqrt{\det R \det R^T}} \det Q \det R$$

$$= \frac{1}{\sqrt{(\det R)^2}} \det Q \det R = \det Q = 1,$$

since $Q \in SO(3)$. Since $\mathscr{J}$ is a Morse function, its critical points are non-degenerate. Due to the Morse lemma [16], these critical points are isolated, and hence the estimate given by (3) is uniquely minimizing. $\square$

It would be pertinent to mention here that there are a total of eight critical points of the function $\mathscr{J} : SO(3) \to \mathbb{R}$ depending on the different sign permutations of the three real eigenvalues of the symmetric matrix S; these permutations are $(-,-,-)$, $(-,-,+)$, $(-,+,-)$, $(+,-,-)$, $(+,+,-)$, $(+,-,+)$, $(-,+,+)$, and $(+,+,+)$. The last of these permutations gives rise to a positive definite S that results in the absolute minimum of $\mathscr{J}$ over $SO(3)$.

2.2. State bounding estimation

Here we discuss the general idea of deterministic state bounding estimation, using ellipsoidal sets to describe state uncertainty and measurement noise. A stochastic state estimator requires probabilistic models for the state uncertainty and the noise. However, statistical properties of the uncertainty and the noise are often not available. We usually make statistical assumptions on disturbance and noise in order to make the estimation problem mathematically tractable. In many practical situations such idealized assumptions are not appropriate, and this may cause poor estimation performance [26].

An alternative deterministic approach is to specify bounds on the uncertainty and the measurement noise without any

assumption on its distribution. Noise bounds are available in many cases, and deterministic estimation is robust to the noise distribution. An efficient but flexible way to describe the bounds is using ellipsoidal sets, referred to as uncertainty ellipsoids.

The deterministic estimation process using uncertainty ellipsoids has the same structure as the Kalman filter. This deterministic estimation procedure is illustrated in Fig. 1, where the figure on the left shows evolution of an uncertainty ellipsoid in time, and the figure on the right shows a cross-section at a fixed time when the state is measured. Suppose that the time interval between two sets of measurements is divided into l equal time steps for discrete integration, and the subscript k denotes the kth discrete integration time step. At the previous measurement instant, corresponding to the kth time step, the state is bounded by an uncertainty ellipsoid centered at the estimated state $\hat{x}_k$. This initial ellipsoid and the estimated state at its center are propagated through time. Depending on the dynamics of the system, the size and the shape of the tube are changed. The new set of measurements are taken at the $(k+l)$th time step. At the $(k+l)$th time step, the predicted uncertainty ellipsoid is centered at $\hat{x}_{k+l}^f$. Another ellipsoidal bound on the state is obtained from the measurements. The measured uncertainty ellipsoid is centered at $\hat{x}_{k+l}^m$. The state lies in the intersection of the two ellipsoids. In the estimation procedure, we find the smallest ellipsoid that contains this intersection, which is shown in the right figure. The center of the new ellipsoid, $\hat{x}_{k+l}$ is considered as a point estimate at time step $k + l$, and the magnitude of the new uncertainty ellipsoid measures the accuracy of the estimation. If the size of the uncertainty ellipsoid is small, then we can conclude that the estimated state is accurate. The deterministic estimation is optimal in the sense that the size of the new ellipsoid is minimized.

The deterministic estimation process is based on the state estimation techniques developed in [23]. Optimal deterministic state or parameter estimation is considered in [9,15,18], where an analytic solution for the minimum ellipsoid that contains a union or an intersection of ellipsoids is given. Parameter estimation in the presence of bounded noise is dealt with in [1,4].

2.3. Attitude estimation problem formulation

2.3.1. Equations of motion

We consider estimation of the attitude dynamics of a rigid body in the presence of an attitude dependent potential. We assume that the potential $U(\cdot) : SO(3) \mapsto \mathbb{R}$ is determined by the attitude of the rigid body, $C \in SO(3)$. A spacecraft on a circular orbit including gravity gradient effects [13], or a 3D pendulum [12] can be modeled in this way. The continuous equations of motion are given by

$$J\dot{\omega} + \omega \times J\omega = M, \qquad (6)$$

$$\dot{C} = CS(\omega), \qquad (7)$$

where $J \in \mathbb{R}^{3\times3}$ is the moment of inertia matrix of the rigid body, $\omega \in \mathbb{R}^3$ is the angular velocity of the body expressed in the body fixed frame, and $S(\cdot) : \mathbb{R}^3 \mapsto so(3)$ is a skew mapping defined such that $S(x)y = x \times y$ for all $x, y \in \mathbb{R}^3$. $M \in \mathbb{R}^3$ is the moment due to the potential. The moment is determined by the relationship, $S(M) = \frac{\partial U}{\partial C}^{\mathrm{T}} C - C^{\mathrm{T}} \frac{\partial U}{\partial C}$, or more explicitly,

$$M = r_1 \times v_{r_1} + r_2 \times v_{r_2} + r_3 \times v_{r_3}, \qquad (8)$$

where $r_i, v_{r_i} \in \mathbb{R}^{1\times3}$ are the ith row vectors of C and $\partial U/\partial C$, respectively. Here the matrix $\partial U/\partial C \in \mathbb{R}^{3\times3}$ is defined such that $[\partial U/\partial C]_{ij} = \partial U/\partial[C]_{ij}$ for $i, j \in (1, 2, 3)$, where $[A]_{ij}$ denote the (i, j)th element of a matrix A. The detailed description of this rigid body model and the derivation of the above equations can be found in [12].

General numerical integration methods, including the popular Runge–Kutta schemes, typically preserve neither first integrals nor the characteristics of the configuration space, $SO(3)$. In particular, the orthogonal structure of the rotation matrices is not preserved numerically. It is often proposed to parameterize (7) by Euler angles or quaternions instead of integrating (7) directly. However, Euler angles have singularities. The numerical simulation process has to be monitored and switching between Euler angle charts is necessary in order to avoid singularities. Quaternions are free of singularities, but the quaternion representing the attitude is required to have unit length. The matrix corresponding to a quaternion which is not of unit length is not orthogonal, and hence does not represent a rotation.

To resolve these problems, a Lie group variational integrator for the attitude dynamics of a rigid body is proposed in [12]. This Lie group variational integrator is described by the discrete time equations.

$$hS\left(J\omega_k + \frac{h}{2}M_k\right) = F_k J_d - J_d F_k^{\mathrm{T}}, \qquad (9)$$

$$C_{k+1} = C_k F_k, \qquad (10)$$

$$J\omega_{k+1} = F_k^{\mathrm{T}} J\omega_k + \frac{h}{2} F_k^{\mathrm{T}} M_k + \frac{h}{2} M_{k+1}, \qquad (11)$$

where $J_d \in \mathbb{R}^3$ is a non-standard moment of inertia matrix defined by $J_d = \frac{1}{2}\mathrm{tr}[J]I_{3\times3} - J$, and $F_k \in SO(3)$ is the relative attitude over an integration step. The constant $h \in \mathbb{R}^+$ is the integration step size. This integrator yields a map

$(C_k, \omega_k) \mapsto (C_{k+1}, \omega_{k+1})$ by solving (9) to obtain $F_k \in SO(3)$ and substituting it into (10) and (11) to obtain C_{k+1} and ω_{k+1}. Numerically, we ensure that F_k remains on $SO(3)$ by requiring that $F_k = \exp(S(f_k))$, where $f_k \in \mathbb{R}^3$. This allows us to express the discrete equations in terms of $f_k \in \mathbb{R}^3$ as opposed to $F_k \in SO(3)$.

Since this integrator does not use a local parameterization, the attitude is defined globally without singularities. It preserves the orthogonal structure of $SO(3)$ because the rotation matrix is updated by a multiplication of two rotation matrices in (10), which is a group operation of $SO(3)$. This integrator is obtained from a discrete variational principle, and it exhibits the characteristic symplectic and momentum preservation properties, and good energy behavior characteristic of variational integrators. We use (9), (10), and (11) in the following development of the attitude estimator.

2.3.2. Uncertainty ellipsoid

An uncertainty ellipsoid in $\mathbb{R}^n$ is defined as

$$\mathscr{E}_{\mathbb{R}^n}(\hat{x}, P) = \{x \in \mathbb{R}^n | (x - \hat{x})^{\mathrm{T}} P^{-1} (x - \hat{x}) \leqslant 1\}, \qquad (12)$$

where $\hat{x} \in \mathbb{R}^n$ and $P \in \mathbb{R}^{n\times n}$ is a symmetric positive definite matrix. We call $\hat{x}$ the center of the uncertainty ellipsoid, and we call P the uncertainty matrix that determines the size and the shape of the uncertainty ellipsoid. The size of an uncertainty ellipsoid is measured by $\mathrm{tr}[P]$. It equals the sum of the squares of the semi principal axes of the ellipsoid.

The configuration space of the attitude dynamics is $SO(3)$, so the state evolves in the 6 D tangent bundle, $TSO(3)$. The corresponding uncertainty ellipsoid is a submanifold of $TSO(3)$.

We obtain the diffeomorphism $TSO(3) \simeq SO(3) \times so(3)$ by left trivialization, and the diffeomorphism $S(\cdot) : \mathbb{R}^3 \mapsto so(3)$ identifies $so(3)$ and $\mathbb{R}^3$. Therefore, $TSO(3) \simeq SO(3) \times \mathbb{R}^3$. For the remainder of the paper, we will represent the state as an element of $SO(3) \times \mathbb{R}^3$. An uncertainty ellipsoid centered at $(\hat{C}, \hat{\omega})$ is induced from an uncertainty ellipsoid in $\mathbb{R}^6$, using the Lie algebra $so(3)$;

$$\mathscr{E}(\hat{C}, \hat{\omega}, P)$$
$$= \left\{ C \in SO(3), \, \omega \in \mathbb{R}^3 \, \middle| \begin{bmatrix} \zeta \\ \delta\omega \end{bmatrix} \in \mathscr{E}_{\mathbb{R}^6}(0_6, P) \right\}, \qquad (13)$$

where $S(\zeta) = \log \mathrm{m}(\hat{C}^{\mathrm{T}} C) \in so(3)$, $\delta\omega = \omega - \hat{\omega} \in \mathbb{R}^3$, and $P \in \mathbb{R}^{6\times6}$ is a symmetric positive definite matrix. Equivalently, an element $(C, \omega) \in \mathscr{E}(\hat{C}, \hat{\omega}, P)$ can be written as

$$C = \hat{C} \exp(S(\zeta)),$$

$$\omega = \hat{\omega} + \delta\omega$$

for some $x = [\zeta^{\mathrm{T}}, \, \delta\omega^{\mathrm{T}}]^{\mathrm{T}} \in \mathbb{R}^6$ satisfying $x^{\mathrm{T}} P^{-1} x \leqslant 1$.

2.3.3. Uncertainty model

We describe the measurement error models for the measured direction vectors and the angular velocity. The direction vector $b^i \in \mathbb{S}^2$ is measured in the body fixed frame, and let $\tilde{b}^i \in \mathbb{S}^2$ denote the measured direction. Since we only measure directions, we normalize b^i and $\tilde{b}^i$ so that they have unit lengths.

Therefore it is inappropriate to express the measurement error by a vector difference. The measurement error is modeled by rotation of the measured direction;

$$b^i = \exp(S(v^i))\tilde{b}^i$$
$$\simeq \tilde{b}^i + S(v^i)\tilde{b}^i, \tag{14}$$

where $v^i \in \mathbb{R}^3$ is the measurement error, which represents the Euler axis of rotation vector from $\tilde{b}^i$ to b^i, and $\|v^i\|$ is the corresponding rotation angle in radians. We assume that the measurement error is small to obtain the second equality.

The angular velocity measurement errors are modeled as

$$\omega = \tilde{\omega} + \upsilon, \tag{15}$$

where $\tilde{\omega} \in \mathbb{R}^3$ is the measured angular velocity and $\upsilon \in \mathbb{R}^3$ is an additive measurement error.

We assume that the initial conditions and the measurement error are bounded by prescribed uncertainty ellipsoids.

$$(C_0, \omega_0) \in \mathscr{E}(\hat{C}_0, \hat{\omega}_0, P_0), \tag{16}$$

$$v^i \in \mathscr{E}_{\mathbb{R}^3}(0, S^i), \tag{17}$$

$$\upsilon \in \mathscr{E}_{\mathbb{R}^3}(0, T), \tag{18}$$

where $P_0 \in \mathbb{R}^{6\times6}$ and $S^i, T \in \mathbb{R}^{3\times3}$ are symmetric positive definite matrices that define the shape and the size of the uncertainty ellipsoids.

3. Attitude estimation with angular velocity measurements

In this section, we develop a deterministic estimator for the attitude and the angular velocity of a rigid body assuming that both the attitude measurement and the angular velocity measurements are available. The estimation process consists of three stages; flow update, measurement update, and filtering. The flow update predicts the uncertainty ellipsoid in the future. The measurement update finds an uncertainty ellipsoid in the state space using the measurements and the measurement error model. The filtering stage obtains a new uncertainty ellipsoid compatible with the predicted uncertainty ellipsoid and the measured uncertainty ellipsoid.

The superscript i denotes the ith directional measurement. The superscript f denotes variables related to the flow update, while the superscript m denotes variables related to the measurement update. The notation $\tilde{\cdot}$ denotes a measured variable, while $\hat{\cdot}$ denotes an estimated variable.

3.1. Flow update

Suppose that the attitude and the angular momentum at the kth step, which corresponds to the previous measurement instant, lie in a given uncertainty ellipsoid:

$$(C_k, \omega_k) \in \mathscr{E}(\hat{C}_k, \hat{\omega}_k, P_k).$$

The flow update gives us the center and the uncertainty matrix that define the uncertainty ellipsoid at the $(k + l)$th step (the current measurement instant) using the given uncertainty ellipsoid at the kth step. Since the attitude dynamics of a rigid body is nonlinear, the boundary of the state at the $(k+l)$th step is not an ellipsoid in general. We assume that the given uncertainty ellipsoid at the kth step is sufficiently small that the states in the uncertainty ellipsoids can be approximated by linearized equations of motion. Then we can guarantee that the boundary of the state at the $(k + l)$th step is an ellipsoid, and we can compute the center and the uncertainty matrix at the $(k + l)$th step separately.

Center: For the given center, $(\hat{C}_k, \hat{\omega}_k)$, the center of the uncertainty ellipsoid due to flow propagation is denoted $(\hat{C}_{k+1}^f, \hat{\omega}_{k+1}^f)$. This center is obtained from the discrete equations of motion, (9), (10), and (11) applied to $(\hat{C}_k, \hat{\omega}_k)$:

$$hS\left(J\hat{\omega}_k + \frac{h}{2}\hat{M}_k\right) = \hat{F}_k J_d - J_d \hat{F}_k^{\mathrm{T}}, \tag{19}$$

$$\hat{C}_{k+1}^f = \hat{C}_k \hat{F}_k, \tag{20}$$

$$J\hat{\omega}_{k+1}^f = \hat{F}_k^{\mathrm{T}} J\hat{\omega}_k + \frac{h}{2}\hat{F}_k^{\mathrm{T}}\hat{M}_k + \frac{h}{2}\hat{M}_{k+1}. \tag{21}$$

This integrator yields a map $(\hat{C}_k, \hat{\omega}_k) \mapsto (\hat{C}_{k+1}^f, \hat{\omega}_{k+1}^f)$, and this process can be repeated to find the center at the $(k + l)$th step, $(\hat{C}_{k+l}^f, \hat{\omega}_{k+l}^f)$.

Uncertainty matrix: We assume that an uncertainty ellipsoid contains small perturbations from its center. Then the uncertainty matrix is obtained by linearizing the above discrete equations of motion. At the $(k + 1)$th step, the uncertainty ellipsoid is represented by perturbations from the center $(\hat{C}_{k+l}^f, \hat{\omega}_{k+l}^f)$ as

$$C_{k+1} = \hat{C}_{k+1}^f \exp(S(\zeta_{k+1}^f)),$$

$$\omega_{k+1} = \hat{\omega}_{k+1}^f + \delta\omega_{k+1}^f$$

for some $\zeta_{k+1}^f, \delta\omega_{k+1}^f \in \mathbb{R}^3$. The uncertainty matrix at the $(k + 1)$th step is obtained by finding a bound on $\zeta_{k+1}^f, \delta\omega_{k+1}^f \in \mathbb{R}^3$. Assume that the uncertainty ellipsoid at the kth step is sufficiently small. Then, $\zeta_{k+1}^f, \delta\omega_{k+1}^f$ are represented by the following linear equations (using the results presented in [13]):

$$x_{k+1}^f = A_k^f x_k,$$

where $x_k = [\zeta_k^{\mathrm{T}}, \delta\omega_k^{\mathrm{T}}]^{\mathrm{T}} \in \mathbb{R}^6$, and $A_k^f \in \mathbb{R}^{6\times6}$ can be suitably defined. Since $(C_k, \omega_k) \in \mathscr{E}(\hat{C}_k, \hat{\omega}_k, P_k)$, $x_k \in \mathscr{E}_{\mathbb{R}^6}(0, P_k)$ by the definition of the uncertainty ellipsoid given in (13). Then we can show that $A_k^f x_k$ lies in the following uncertainty ellipsoid.

$$A_k^f x_k \in \mathscr{E}_{\mathbb{R}^6}(0, A_k^f P_k (A_k^f)^{\mathrm{T}}).$$

Thus, the uncertainty matrix at the $(k + 1)$th step is given by

$$P_{k+1}^f = A_k^f P_k (A_k^f)^{\mathrm{T}}. \tag{22}$$

The above equation can be applied repeatedly to find the uncertainty matrix at the $(k + l)$th step.

We have obtained expressions to predict the center and the uncertainty matrix in the future from the current uncertainty

ellipsoid using the discrete flow. In summary, the uncertainty ellipsoid at the $(k+l)$th step is computed using (19), (20), (21), and (22) as:

$$(C_{k+l}, \omega_{k+l}) \in \mathscr{E}(\hat{C}^f_{k+l}, \hat{\omega}^f_{k+l}, P^f_{k+l}),$$
$$P^f_{k+l} = A^f P_k (A^f_k)^{\mathrm{T}}, \tag{23}$$

where $A^f = A^f_{k+l-1} A^f_{k+l-2} \cdots A^f_k \in \mathbb{R}^{6\times6}$.

3.2. Measurement update

We assume that the attitude and the angular velocity of a rigid body are measured simultaneously. The measured attitude and the measured angular velocity have uncertainties since the measurements contain measurement errors. However, we can find bounds for the actual state because the measurement errors are bounded by known uncertainty ellipsoids given by (17) and (18). The measurement update stage finds an uncertainty ellipsoid in the state space using the measurements and the measurement error models. The measured attitude and the measured angular velocity are the center of the measured uncertainty ellipsoid, and the measurement error models are used to find the uncertainty matrix.

Center: The center of the uncertainty ellipsoid, $(\hat{C}^m_{k+l}, \hat{\omega}^m_{k+l})$ is obtained by measurements. The attitude is determined by measuring the directions to the known points in the inertial frame. Let the measured directions to the known points be $\tilde{B}_{k+l} = [\tilde{b}^1, \tilde{b}^2, \ldots, \tilde{b}^m] \in \mathbb{R}^{3\times m}$. Then, the attitude $\hat{C}^m_{k+l}$ satisfies the following necessary condition given in (2):

$$(\hat{C}^m_{k+l})^{\mathrm{T}} \tilde{L}_{k+l} - \tilde{L}^{\mathrm{T}}_{k+l} \hat{C}^m_{k+l} = 0, \tag{24}$$

where $\tilde{L}_{k+l} = E_{k+l} W_{k+l} \tilde{B}^{\mathrm{T}}_{k+l} \in \mathbb{R}^{3\times3}$. The solution of (24) is obtained by a QR factorization of $\tilde{L}_{k+l}$ as given in Theorem 2.1

$$\hat{C}^m_{k+l} = \left(Q_q \sqrt{(Q_r Q^{\mathrm{T}}_r)^{-1}} Q^{\mathrm{T}}_q \right) \tilde{L}_{k+l}, \tag{25}$$

where $Q_q \in \mathrm{SO}(3)$ is an orthogonal matrix and $Q_r \in \mathbb{R}^{3\times3}$ is an upper triangular matrix satisfying $\tilde{L}_{k+l} = Q_q Q_r$.

The angular velocity is measured directly,

$$\hat{\omega}^m_{k+l} = \tilde{\omega}_{k+l}. \tag{26}$$

Uncertainty matrix: We can represent the actual state at the $(k+l)$th step using the measured center and perturbations as follows:

$$C_{k+l} = \hat{C}^m_{k+l} \exp(S(\zeta^m_{k+l})), \tag{27}$$

$$\omega_{k+l} = \hat{\omega}^m_{k+l} + \delta\omega^m_{k+l} \tag{28}$$

for $\zeta^m_{k+l}, \delta\omega^m_{k+l} \in \mathbb{R}^3$. The uncertainty matrix is obtained by finding an ellipsoid containing $\zeta^m_{k+l}, \delta\omega^m_{k+l}$.

We determine the attitude indirectly by comparing the known directions in the reference frame with measurements in the body frame. So, we need to transform the uncertainties in the direction measurements into the uncertainties in the rotation matrix by (24). Using the measurement error model defined in (14), the actual direction matrix to the known point B_{k+l} is given by

$$B_{k+l} = \tilde{B}_{k+l} + \delta\tilde{B}_{k+l}, \tag{29}$$

where $\delta B_{k+l} = [S(v^1)\tilde{b}^1, S(v^2)\tilde{b}^2, \ldots, S(v^m)\tilde{b}^m] \in \mathbb{R}^{3\times m}$.

The actual matrix giving the known directions B_{k+l} and the actual attitude C_{k+l} at the $(k+l)$th step also satisfy (25);

$$C^{\mathrm{T}}_{k+l} L_{k+l} - L^{\mathrm{T}}_{k+l} C_{k+l} = 0, \tag{30}$$

where $L_{k+l} = E_{k+l} W_{k+l} B^{\mathrm{T}}_{k+l} \in \mathbb{R}^{3\times3}$. Substituting (27) and (29) into (30), and assuming that the size of the measurement error is sufficiently small, the above equation can be written as

$$\tilde{L}^{\mathrm{T}}_{k+l} \hat{C}^m_{k+l} S(\zeta^m_{k+l}) + S(\zeta^m_{k+l})(\hat{C}^m_{k+l})^{\mathrm{T}} \tilde{L}_{k+l}$$
$$= (\hat{C}^m_{k+l})^{\mathrm{T}} E_{k+l} W_{k+l} \delta B^{\mathrm{T}}_{k+l} - \delta B_{k+l} W_{k+l} E^{\mathrm{T}}_{k+l} \hat{C}^m_{k+l}.$$

Using the identity, $S(x)A + A^{\mathrm{T}}S(x) = S(\{\mathrm{tr}[A]I_{3\times3} - A\}x)$ for $A \in \mathbb{R}^{3\times3}$, $x \in \mathbb{R}^3$, the above equation can be written in a vector form.

$$\{\mathrm{tr}[(\hat{C}^m_{k+l})^{\mathrm{T}} \tilde{L}_{k+l}] - (\hat{C}^m_{k+l})^{\mathrm{T}} \tilde{L}_{k+l}\}\zeta^m_{k+l}$$
$$= -\sum_{i=1}^{m} w_i \{\mathrm{tr}[\tilde{b}^i (e^i)^{\mathrm{T}} \hat{C}^m_{k+l}] I_{3\times3} - \tilde{b}^i (e^i)^{\mathrm{T}} \hat{C}^m_{k+l}\}v^i.$$

Then, we obtain

$$\zeta^m_{k+l} = \sum_{i=1}^{m} \mathscr{A}^{m,i}_{k+l} v^i, \tag{31}$$

where

$$\mathscr{A}^{m,i}_{k+l} = -\{\mathrm{tr}[(\hat{C}^m_{k+l})^{\mathrm{T}} \tilde{L}_{k+l}] - (\hat{C}^m_{k+l})^{\mathrm{T}} \tilde{L}_{k+l}\}^{-1}$$
$$w_i \{\mathrm{tr}[\tilde{b}^i (e^i)^{\mathrm{T}} \hat{C}^m_{k+l}] I_{3\times3} - \tilde{b}^i (e^i)^{\mathrm{T}} \hat{C}^m_{k+l}\}. \tag{32}$$

This equation expresses the uncertainty in the measured attitude as a linear combination of the directional measurement errors.

The perturbation of the angular velocity $\delta\omega^m_{k+l}$ is equal to the angular velocity measurement error v_{k+l}, since we measure the angular velocity directly. Substituting (28) into (15), we obtain

$$\delta\omega^m_{k+l} = v_{k+l}. \tag{33}$$

Define $x^m_{k+l} = [(\zeta^m_{k+l})^{\mathrm{T}}, (\delta\omega^m_{k+l})^{\mathrm{T}}]^{\mathrm{T}} \in \mathbb{R}^6$. Using (31) and (33),

$$x^m_{k+l} = H_1 \sum_{i=1}^{m} \mathscr{A}^{m,i}_{k+l} v^i_{k+l} + H_2 v_{k+l},$$

where $H_1 = [I_{3\times3}, 0_{3\times3}]^{\mathrm{T}}, H_2 = [0_{3\times3}, I_{3\times3}]^{\mathrm{T}} \in \mathbb{R}^{6\times3}$. Now x^m_{k+l} is expressed as a linear combination of the measurement errors v^i and v. Using (17) and (18), we can show that each term in the right-hand side of the above equation is in the following uncertainty ellipsoids:

$$H_1 \mathscr{A}^{m,i}_{k+l} v^i_{k+l} \in \mathscr{E}_{\mathbb{R}^6}(0, H_1 \mathscr{A}^{m,i}_{k+l} S^i_{k+l} (\mathscr{A}^{m,i}_{k+l})^{\mathrm{T}} H^{\mathrm{T}}_1),$$

$$H_2 v_{k+l} \in \mathscr{E}_{\mathbb{R}^6}(0, H_2 T_{k+l} H^{\mathrm{T}}_2).$$

Thus, the uncertainty ellipsoid for x^m_{k+l} is obtained as the vector sum of the above uncertainty ellipsoids. The measurement

update procedure is to find a minimal ellipsoid that contains the vector sum of those uncertainty ellipsoids. Expressions for a minimal ellipsoid containing the vector sum of multiple ellipsoids are presented in [15] and [9]. Using the results, we obtain

$$
P_{k+l}^m = \left\{ \sum_{i=1}^m \sqrt{\text{tr}[H_1 \mathscr{A}_{k+l}^{m,i} S_{k+l}^i (\mathscr{A}_{k+l}^{m,i})^{\text{T}} H_1^{\text{T}}]} \right.
$$
$$
+ \sqrt{\text{tr}[H_2 T_{k+l} H_2^{\text{T}}]} \Bigg\}
$$
$$
\times \left\{ \sum_{i=1}^m \frac{H_1 \mathscr{A}_{k+l}^{m,i} S_{k+l}^i (\mathscr{A}_{k+l}^{m,i})^{\text{T}} H_1^{\text{T}}}{\sqrt{\text{tr}[H_1 \mathscr{A}_{k+l}^{m,i} S_{k+l}^i (\mathscr{A}_{k+l}^{m,i})^{\text{T}} H_1^{\text{T}}]}} \right.
$$
$$
\left. + \frac{H_2 T_{k+l} H_2^{\text{T}}}{\sqrt{\text{tr}[H_2 T_{k+l} H_2^{\text{T}}]}} \right\}. \tag{34}
$$

In summary, the measured uncertainty ellipsoid at the $(k+l)$th step is defined by (25), (26), and (34);

$$
(C_{k+l}, \omega_{k+l}) \in \mathscr{E}(\hat{C}_{k+l}^m, \hat{\omega}_{k+l}^m, P_{k+l}^m). \tag{35}
$$

3.3. Filtering procedure

The filtering procedure is to find a new uncertainty ellipsoid compatible with both the predicted uncertainty ellipsoid and the measured uncertainty ellipsoid. From (23) and (35), we know that the state at $(k+l)$th step lies in the intersection of the two uncertainty ellipsoids:

$$
(C_{k+l}, \omega_{k+l}) \in \mathscr{E}(\hat{C}_{k+l}^f, \hat{\omega}_{k+l}^f, P_{k+l}^f)
$$
$$
\cap \mathscr{E}(\hat{C}_{k+l}^m, \hat{\omega}_{k+l}^m, P_{k+l}^m). \tag{36}
$$

However, the intersection of two ellipsoids is not generally an ellipsoid. We find a minimal uncertainty ellipsoid containing this intersection. We first obtain equivalent uncertainty ellipsoids in $\mathbb{R}^6$, and convert them to uncertainty ellipsoids in TSO(3). We omit the subscript $(k+l)$ in this subsection for convenience.

The uncertainty ellipsoid obtained from the measurements, $\mathscr{E}(\hat{C}^m, \hat{\omega}^m, P^m)$, is identified by its center $(\hat{C}^m, \hat{\omega}^m)$, and the uncertainty ellipsoid in $\mathbb{R}^6$:

$$
(\zeta^m, \delta\omega^m) \in \mathscr{E}_{\mathbb{R}^6}(0_{6\times 1}, P^m), \tag{37}
$$

where $S(\zeta^m) = \log m(\hat{C}^{m,T} C) \in \mathfrak{so}(3)$, $\delta\omega^m = \omega - \hat{\omega}^m \in \mathbb{R}^3$. Similarly, the uncertainty ellipsoid obtained from the flow update, $\mathscr{E}(\hat{C}^f, \hat{\omega}^f, P^f)$, is identified by its center $(\hat{C}^f, \hat{\omega}^f)$, and the uncertainty ellipsoid in $\mathbb{R}^6$.

$$
(\zeta^f, \delta\omega^f) \in \mathscr{E}_{\mathbb{R}^6}(0_{6\times 1}, P^f), \tag{38}
$$

where $S(\zeta^f) = \log m(\hat{C}^{f,T} C) \in \mathfrak{so}(3)$, $\delta\omega^f = \omega - \hat{\omega}^f \in \mathbb{R}^3$. Equivalently, an element $(C^f, \omega^f) \in \mathscr{E}(\hat{C}^f, \hat{\omega}^f, P^f)$, is given by

$$
C^f = \hat{C}^f \exp(S(\zeta^f)), \tag{39}
$$

$$
\omega^f = \hat{\omega}^f + \delta\omega^f, \tag{40}
$$

for some $(\zeta^f, \delta\omega^f) \in \mathscr{E}_{\mathbb{R}^6}(0_{6\times 1}, P^f)$. We find an equivalent expression for (38) based on the center $(\hat{C}^m, \hat{\omega}^m)$ obtained from the measurements.

Define $\hat{\zeta}^{mf}, \delta\hat{\omega}^{mf} \in \mathbb{R}^3$ such that

$$
\hat{C}^f = \hat{C}^m \exp(S(\hat{\zeta}^{mf})), \tag{41}
$$

$$
\hat{\omega}^f = \hat{\omega}^m + \delta\hat{\omega}^{mf}. \tag{42}
$$

Thus, $\hat{\zeta}^{mf}, \delta\hat{\omega}^{mf}$ represent the difference between the centers of the two ellipsoids.

Substituting (41), (42) into (39), (40), we obtain

$$
C^f = \hat{C}^m \exp(S(\hat{\zeta}^{mf})) \exp(S(\zeta^f)),
$$
$$
\simeq \hat{C}^m \exp(S(\hat{\zeta}^{mf} + \zeta^f)), \tag{43}
$$

$$
\omega^f = \hat{\omega}^m + (\delta\hat{\omega}^{mf} + \delta\omega^f), \tag{44}
$$

where we assumed that $\hat{\zeta}^{mf}, \zeta^f$ are sufficiently small to obtain the second equality. Thus, the uncertainty ellipsoid obtained by the flow update, $\mathscr{E}(\hat{C}^f, \hat{\omega}^f, P^f)$, is described by the center $(\hat{C}^m, \hat{\omega}^m)$ obtained from the measurement and the following uncertainty ellipsoid in $\mathbb{R}^6$:

$$
\mathscr{E}_{\mathbb{R}^6}(\hat{x}^{mf}, P^f), \tag{45}
$$

where $\hat{x}^{mf} = [(\hat{\zeta}^{mf})^{\text{T}}, (\delta\hat{\omega}^{mf})^{\text{T}}]^{\text{T}} \in \mathbb{R}^6$.

We seek a minimal ellipsoid that contains the intersection of two uncertainty ellipsoids in $\mathbb{R}^6$.

$$
\mathscr{E}_{\mathbb{R}^6}(0_{6\times 1}, P^m) \cap \mathscr{E}_{\mathbb{R}^6}(\hat{x}^{mf}, P^f) \subset \mathscr{E}_{\mathbb{R}^6}(\hat{x}, P), \tag{46}
$$

where $\hat{x} = [\hat{\zeta}^{\text{T}}, \delta\hat{\omega}^{\text{T}}]^{\text{T}} \in \mathbb{R}^6$. Using the result presented in [15], $\hat{x}$ and P can be written as

$$
\hat{x} = L\hat{x}^{mf}, \quad P = \beta(q)(I - L)P^m, \tag{47}
$$

where

$$
\beta(q) = 1 + q - (\hat{x}^{mf})^{\text{T}} (P^m)^{-1} L\hat{x}^{mf}, \tag{48}
$$

$$
L = P^m (P^m + q^{-1} P^f)^{-1}. \tag{49}
$$

The constant $q \geq 0$ is chosen such that $\text{tr}[P]$ is minimized. We convert $\hat{x}$ to points in TSO(3) using the common center $(\hat{C}^m, \hat{\omega}^m)$.

In summary, the attitude estimation filter algorithm is given by the following statement.

Proposition 3.1. *The attitude and angular velocity estimates and the new uncertainty ellipsoid at the $(k+l)$th step are given by*

$$
\hat{C}_{k+l} = \hat{C}_{k+l}^m \exp(S(\hat{\zeta})), \tag{50}
$$

$$
\hat{\omega}_{k+l} = \hat{\omega}_{k+l}^m + \delta\hat{\omega}, \tag{51}
$$

$$
P_{k+l} = P, \tag{52}
$$

where $\hat{x} = [\hat{\zeta}^T, \delta\hat{\omega}^T]^T \in \mathbb{R}^6$ and $P \in \mathbb{R}^{6\times 6}$ are given by Eqs. (47)–(49). The actual state lies in the ellipsoid

$$(C_{k+l}, \omega_{k+l}) \in \mathscr{E}(\hat{C}_{k+l}, \hat{\omega}_{k+l}, P_{k+l}), \tag{53}$$

centered at the estimated attitude and angular velocity states.

Remark. For the approximation given in (43), we assume that $\hat{\zeta}^{mf}, \zeta^f$ are sufficiently small. This assumption can be avoided if we use the Baker–Campbell–Hausdorff formula given by

$$\exp(S(\hat{\zeta}^{mf}))\exp(S(\zeta^f)) = \exp(S(\mathrm{BCH}(\hat{\zeta}^{mf}, \zeta^f))),$$

where the explicit expression for $\mathrm{BCH} : \mathbb{R}^3 \times \mathbb{R}^3 \mapsto \mathbb{R}^3$ can be found in [10]. Then, instead of (45), the uncertainty ellipsoid obtained by the flow update is described by the center $(\hat{C}^m, \hat{\omega}^m)$ obtained from the measurement and the uncertainty ellipsoid in $\mathbb{R}^6$, $\mathscr{E}_{\mathbb{R}^6}(\hat{y}^{mf}, Q^f)$, where the expressions for $\hat{y}^{mf} \in \mathbb{R}^6$ and a symmetric positive definite $Q^f \in \mathbb{R}^{6\times 6}$ are given by the solution of the following optimization problem.

for given $\hat{\zeta}^{mf}, \delta\hat{\omega}^{mf}, P^f$,

$$\min_{\hat{y}^{mf}, Q^f} \mathrm{tr}[Q^f],$$

such that $[\mathrm{BCH}(\hat{\zeta}^{mf}, \zeta^f)^T, (\delta\hat{\omega}^{mf} + \delta\omega^f)^T]^T$
$$\in \mathscr{E}_{\mathbb{R}^6}(\hat{y}^{mf}, Q^f),$$

for any $[\zeta^f, \delta\omega^f] \in \mathscr{E}_{\mathbb{R}^6}(0_6, P^f)$.

This optimization problem can be solved numerically using computational methods for finding minimum volume ellipsoids covering a finite set, given in [6], by discretizing the uncertainty ellipsoid $\mathscr{E}_{\mathbb{R}^6}(0_6, P^f)$. However, the resulting computational burden could decrease the speed of the estimation algorithm, which would be detrimental for real-time implementation.

The center of the new uncertainty ellipsoid is the estimated state, considered as point estimates of the attitude and the angular velocity at the $(k+l)$th step. The uncertainty matrix represents the bounds on the uncertainty of the estimated state. The size of the uncertainty matrix characterizes the accuracy of the estimate. If the size of the uncertainty ellipsoid is small, we conclude that the estimation is accurate. This estimation is optimal in the sense that the size of the new uncertainty ellipsoid is minimized. The uncertainty matrix can also be used to predict the distribution of the uncertainty. The eigenvector of the uncertainty matrix corresponding to the maximum eigenvalue shows the direction of the maximum uncertainty.

3.4. Convergence of filter

We now present a sufficient condition under which this estimation algorithm converges, i.e., the size of the uncertainty matrix decreases monotonically with measurements. The trace of the positive definite uncertainty matrix P is the measure of size used in this analysis.

Theorem 3.1. *The estimation algorithm given by Proposition 3.1 is convergent if there exists a constant $c \in (0, 1)$ such that the following inequality holds for every measurement:*

$$q\,\mathrm{tr}[P^f] + \mathrm{tr}[P^m] < c(1 + q)\mathrm{tr}[P_0], \tag{54}$$

where P_0 denotes the uncertainty matrix of the filtered estimate at the previous measurement instant.

Proof. For convergence, it is sufficient that the filtering process is a contraction mapping, which is to say that $\mathrm{tr}[P] < c\,\mathrm{tr}[P_0]$ where $c \in (0, 1)$ and P_0 denotes the uncertainty matrix of the filtered estimate at the previous measurement instant.

Using the matrix inversion lemma, we can express the uncertainty matrix P given by (47)–(49) as

$$P = \beta(q)(q(P^f)^{-1} + (P^m)^{-1})^{-1}.$$

Now we have

$$\mathrm{tr}[P] = \beta(q)\mathrm{tr}[(q(P^f)^{-1} + (P^m)^{-1})^{-1}].$$

From Eqs. (48)–(49), we have $\beta(q) \leqslant 1 + q$. Thus,

$$\mathrm{tr}[P] \leqslant (1 + q)\mathrm{tr}[(q(P^f)^{-1} + (P^m)^{-1})^{-1}].$$

From Fact 8.10.15 in [5], we know that

$$\mathrm{tr}[(\alpha(P^f)^{-1} + (1-\alpha)(P^m)^{-1})^{-1}] \leqslant \mathrm{tr}[\alpha P^f + (1-\alpha)P^m],$$

for $\alpha \in [0, 1]$, since $(P^f)^{-1}$ and $(P^m)^{-1}$ are positive definite. Since the parameter $q \geqslant 0$, we can substitute $q = \alpha/(1-\alpha)$ for some $\alpha \in [0, 1]$, so that

$$\mathrm{tr}[(q(P^f)^{-1} + (P^m)^{-1})^{-1}]$$
$$= \mathrm{tr}\left[\left\{\frac{1}{1-\alpha}(\alpha(P^f)^{-1} + (1-\alpha)(P^m)^{-1})\right\}^{-1}\right]$$
$$\leqslant (1-\alpha)\mathrm{tr}[\alpha P^f + (1-\alpha)P^m]$$
$$= \alpha(1-\alpha)\mathrm{tr}[P^f] + (1-\alpha)^2\mathrm{tr}[P^m]$$
$$= \frac{q}{(1+q)^2}\mathrm{tr}[P^f] + \frac{1}{(1+q)^2}\mathrm{tr}[P^m].$$

A sufficient condition for convergence for the estimation algorithm is then obtained from the above as:

$$\mathrm{tr}[P] \leqslant (1+q)\mathrm{tr}[(q(P^f)^{-1} + (P^m)^{-1})^{-1}]$$
$$\leqslant \frac{q}{(1+q)}\mathrm{tr}[P^f] + \frac{1}{(1+q)}\mathrm{tr}[P^m] < c\,\mathrm{tr}[P_0],$$

which is equivalent to the sufficient condition (54). $\quad\square$

The rate of convergence is determined by the contraction constant $c \in (0, 1)$ for which the inequality (54) is satisfied for all measurements. This condition shows that having small uncertainties in both measurement and flow propagation facilitates convergence of the filter estimates, as can be expected. It also shows that there is a trade-off between the effects of

the flow induced uncertainty and the measurement uncertainty, given by the parameter q. When q is large, the effect of the flow uncertainty is larger than the measurement uncertainty. The reverse is true when q is small. The limiting cases are (i) when $q = 0$ and (ii) when $q \to \infty$. In the first case, the measurement ellipsoid contains the flow ellipsoid (see [15]) and Theorem 3.1 states that it is sufficient to have $\text{tr}[P^m] < c \, \text{tr}[P_0]$ for convergence. In the second case, the flow ellipsoid contains the measurement ellipsoid (see [15]) and Theorem 3.1 states that it is sufficient to have $\text{tr}[P^f] < c \, \text{tr}[P_0]$ for convergence. For intermediate values of the parameter q, if knowledge of absolute bounds on the size of the flow and measurement uncertainties is available, one can check to see if condition (54) is satisfied, in which case the estimates are guaranteed to converge. However, such knowledge may not always be available a priori. For the special case when the measurement ellipsoid P^m is known a priori or may be assumed constant (i.e., the sensor accuracy remains constant), the sufficient condition (54) provides a bound on the flow uncertainty ellipsoid P^f (or equivalently, a bound on the linear flow matrix A^f). With prior knowledge of the bounds on P^f and P^m and after determining q during the filter step of the estimation scheme, one could also check this condition in real time. One of the important factors that the rate of convergence depends upon is obtained from consideration of the geometry of the intersecting ellipsoids. The rate of convergence depends upon the relative orientation of the major axes of the non-degenerate flow and measurement ellipsoids in the 6D state space. The volume of intersection of these two ellipsoids when their major axes are orthogonal, is smaller than thevolume of intersection when their major axes are closely aligned.

4. Conclusion

A deterministic estimation scheme for the attitude dynamics of a rigid body in an attitude dependent potential field is presented, with an assumption of bounded measurement errors. The properties of the proposed attitude estimation scheme are as follows. This attitude estimator has no singularities since the attitude is represented by a rotation matrix, and the structure of the rotation matrix is preserved since it is updated by group operations in SO(3) using a Lie group variational integrator. The proposed attitude estimator is robust to the distribution of the uncertainty in initial conditions and the measurement noise, since it is a deterministic scheme based on knowledge of the bounds in these uncertainties. A sufficient condition for convergence of this filter has been obtained. These results can be extended in a number of different directions, like: relaxing the assumption that the number of attitude measurements at each measurement step is $m = 3$, eliminating the assumption of velocity measurements at each measurement update step, and adding the effects of process noise.

Acknowledgments

References

[1] E.-W. Bai, K. Nagpal, R. Tempo, Bounded-error parameter estimation: noise models and recursive algorithms, Automatica 32 (7) (1996) 985–999.

[2] I.Y. Bar-Itzhack, Y. Oshman, Attitude determination from vector observations: quaternion estimation, IEEE Trans. Aerospace Electron. Systems 21 (1) (1985) 128–136.

[3] B. Barshan, H.F. Durrant-Whyte, Inertial navigation systems for mobile robots, IEEE Trans. Robotics Automat. 11 (3) (1995) 328–342.

[4] G. Belforte, P. Gay, Optimal worst case estimation for lpv-fir models with bounded errors, Systems Control Lett. 53 (4) (2004) 259–268.

[5] D.S. Bernstein, Matrix Mathematics, Princeton University Press, Princeton, NJ, 2005.

[6] S. Boyd, L.E. Ghaoui, E. Feron, V. Balakrishnan, Linear Matrix Inequalities in System and Control Theory, SIAM, 1994.

[7] J.L. Crassidis, F.L. Markley, A minimum model error approach for attitude estimation, J. Guidance Control Dynamics 20 (6) (1997) 1241–1247.

[8] J.L. Crassidis, F.L. Markley, Unscented filtering for spacecraft attitude estimation, AIAA J. Guidance Control Dynamics 26 (4) (2003) 536–542.

[9] C. Durieu, E. Walter, B. Polyak, Multi-input multi-output ellipsoidal state bounding, J. Optim. Theory Appl. 111 (2) (2001) 273–303.

[10] K. Engø, On the BCH-formula in $\mathfrak{so}(3)$, BIT 41 (3) (2001) 629–631.

[11] J.L. Farrell, J.C. Stuelpnagel, R.H. Wessner, J.R. Velman, J.E. Brock, A least squares estimate of satellite attitude, solution 65-1, SIAM Rev. 8 (3) (1966) 384–386.

[12] T. Lee, M. Leok, N.H. McClamroch, A Lie group variational integrator for the attitude dynamics of a rigid body with applications to the 3D pendulum, in: Proceedings of the IEEE Conference on Control Applications, 2005, pp. 962–967.

[13] T. Lee, M. Leok, N.H. McClamroch, Attitude maneuvers of a rigid spacecraft in a circular orbit, in: Proceedings of the Americal Control Conference, Minneapolis, MN, 2006, pp. 1742–1747.

[14] T. Lee, A.K. Sanyal, M. Leok, N.H. McClamroch, Deterministic global attitude estimation, in: Proceedings of the 45th IEEE Conference on Decision and Control, San Diego, CA, 2006, pp. 3174–3179.

[15] D.G. Maksarov, J.P. Norton, State bounding with ellipsoidal set description of the uncertainty, Internat. J. Control 65 (5) (1996) 847–866.

[16] J. Milnor, Morse Theory, Princeton University Press, Princteon, NJ, 1963.

[17] F.L. Markley, Attitude determination and parameter estimation using vector observations: theory, J. Astronaut. Sci. 37 (6) (1989) 41–58.

[18] B.T. Polyak, S.A. Nazin, C. Durieu, E. Walter, Ellipsoidal parameter or state estimation under model uncertainty, Automatica 40 (7) (2004) 1171–1179.

[19] M.L. Psiaki, Attitude-determination filtering via extended quaternion estimation, AIAA J. Guidance Control Dynamics 23 (2) (2000) 206–214.

[20] H. Rehbinder, X. Hu, Drift-free attitude estimation for accelerated rigid bodies, Automatica 40 (4) (2004) 653–659.

[21] S.I. Roumeliotis, G.S. Sukhatme, G.A. Bekey, Smoother based 3d attitude estimation for mobile robot localization, in: Proceedings of 1999 IEEE International Conference on Robotics and Automation, vol. 3, Detroit, MI, 1999, pp. 1979–1986.

[22] A.K. Sanyal, Optimal attitude estimation and filtering without using local coordinates, Part I: uncontrolled and deterministic attitude dynamics, in: Proceedings of the American Control Conference, Minneapolis, MN, 2006, pp. 5734–5739.

[23] F.C. Schweppe, Recursive state estimation: unknown but bounded errors and system inputs, IEEE Trans. Automat. Control 13 (1) (1968) 22–28.

[24] M.D. Shuster, S.D. Oh, Three-axis attitude determination from vector observations, AIAA J. Guidance Control 4 (1) (1981) 70–77.

[25] M.D. Shuster, Kalman filtering of spacecraft attitude and the quest model, J. Astronaut. Sci. 38 (3) (1990) 377–393.

[26] Y. Theodor, U. Shaked, C.E. de Souza, A game theory approach to robust discrete-time H_∞-estimation, IEEE Trans. Signal Process. 42 (6) (1994) 1486–1495.

[27] J. Vaganay, M.J. Aldon, A. Fournier, Mobile robot attitude estimation by fusion of inertial data, in: Proceedings of the 1993 IEEE International Conference on Robotics and Automation, vol. 1, Atlanta, GA, 1993, pp. 277–282.

[28] G. Wahba, A least squares estimate of satellite attitude, problem 65-1, SIAM Rev. 7 (5) (1965) 409.